

Defect Structure Analysis and Oxygen Nonstoichiometry of Al Substituted SrFeO_{3-δ}

Hanane Fodil^a, mahmoud omari^b, Kaouther El Kourc^c

^aUniversity of Biskra- industrial chemical, Biskra, 07000, Algeria
fodil.hanae@yahoo.fr

^bUniversity of Biskra- matiel science, Biskra, 07000, Algeria

m2omari@yahoo.fr

^cEPSTA School, Algeriers, Algeria
kaouther_youcef@yahoo.fr

^{a,c}Lab:LI3CUB

^bLaboratory of Molecular Chemistry and Environment,

Abstract

A defect chemical model for the behavior of acceptor and donor-doped SrFeO₃ as a function of oxygen pressure is proposed. The non-stoichiometric deviation was calculated as a function of oxygen partial pressure, pO₂, at different temperatures. The mathematical approach allows us to calculate the oxygen partial pressure dependent properties of SrFe_{1-x}Al_xO_{3-δ} in the range 0.10 ≤ x ≤ 0.30. The results show that the conductivity was dependent of pO₂ and proportional to the dopant concentration.

Stability regimes and compensation mechanisms at various oxygen partial pressures and at various temperatures are proposed. This model examines also the charge compensation mechanisms that dominate under the different regimes and their implications for transport properties. From equilibrium constants, Thermodynamic quantities such as standard enthalpy and entropy charge for the defect formation reactions were calculated.

Key words: Defect modeling; SFA ; Non stoichiometry ; Conductivity.

Introduction

Solid oxide fuel cells (SOFCs) are environmentally clean and highly efficient devices used to generate electrochemically. Limited by the oxygen conductivity of the electrolyte, the most operate at about 1000 C°. Such high operating temperatures cause electrode reaction and other engineering difficulties. Many efforts are still under with higher conductivity at lower temperatures.[2][3]

Mizusaki and co-workers studied oxygen non-stoichiometry, diffusion and electrical properties of several perovskite-type with the general formula of LaxSr1-xBO3-δ (B=Al, Zr, Bi, Cr, Mn, Fe, Co) by thermo-gravimetric method and standard four-probe method.[1][4] Carter et al investigated oxygen transport in perovskite-type and the A- and B- site doping effects on conductivity and other properties[5].

For these purposes, the condition behavior under low oxygen pressures must be investigated, since if an appreciable electronic conduction arises as a result of defect equilibrium at low pO₂, the electrical conduction is determined by the concentration of present defects in SFA system. several years ago, spinolo et al[1][2], suggested a general mathematical method to calculate

defect concentrations but without application to actual oxides, A few years later, pulsen[4] has proposed a mathematical approach to calculate the concentration of different species in Ba Fe_{1-x}Al_xO_{3-δ} system.[4]

The purpose of the present work is to establish point defect model equilibrium for SrFe_{1-x}Al_xO_{3-δ} in the range 0 ≤ x ≤ 0.30 using the nonstoichiometry data that were reported by mizisaki et al[19]. The present defect model will allows us to interpret the thermo-gravimetric results in which oxygen vacancies are assumed for the oxygen deficient condition. The relationship between the obtained resulted and those of conductivity measurements [19][20] will also be discussed. Finally from equilibrium constants, thermodynamic quantities such as standard enthalpy and entropy for the defect formation are calculated.

2. Defect chemical model

The defect model proposed here is considered within the regime that corresponds to oxygen deficiency. Only 1 sublattice of SrFe_{1-x}Al_xO_{3-δ} is assumed to be defected. Reduction this system leads to an oxygen deficit in the oxygen sublattice. Interactions between defects and interstitial oxygen are neglected. This model is a random point defect model, based on the presence of 2 oxidation states of iron ions, Fe⁺⁴ and Fe⁺³, that are populated in various proportions depending on temperature, partial pressure of oxygen and Al- doping. It does not take in to account activity coefficients of all present species. The oxygen non-stoichiometry δ assumes negative values, which is explained by the presence of oxide ion vacancies. In the point defect model, the oxygen vacancies are assumed to be fully ionized at high temperatures. In common with earlier work[22][23], this treatment ignores the Schottky defect equilibrium for which, in any case, the equilibrium constant is not available.

For the treatment of point defects in this system we chose the "Kröger-Vink notation"[1][4]. We therefore define vacancies as particles that occupy a defined site in a crystal and that may have a charge. Sites in a crystal are the points where the atoms or the vacancies may be. For a crystal composed of 2 kinds of atoms we have, for example, the "cation sites" and the "oxygen sites". A

point, a negative charge, marks the positive excess charge by a dash to distinguish this relative charge from the absolute charge.

Adopting this type of notation we obtain on the whole a set of independent equations containing the concentrations of the different species (table 1),.

Table 01: Different species used in this defect model with Kroger-vink notation.

Cationic site	anionic sit
Fe(Fe ⁺⁴)	O _o ^x
Fe ^x (Fe ⁺³)	V _O
Sr _{Al} '(Sr ⁺²) Al _{Sr} '(Al ⁺³)	

The charge-neutrality condition leads to

$$2[V_{\text{O}}^{\bullet\bullet}] + [Fe_{Fe}^{\bullet}] = [Sr_{Al}'] \quad (1)$$

The value of $[Al_{Sr}']$ is given by the nominal B site composition x that is

$$[Al_{Sr}'] = x \quad (2)$$

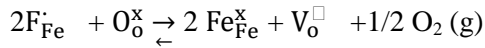
$$[Sr_{Al}'] = 1 \quad (3)$$

Because this solid solution is an oxygen deficient type, we have

$$[V_{\text{O}}^{\bullet\bullet}] = \delta \quad (4)$$

$$[O_{\text{O}}^x] = 3 - \delta \quad (5)$$

The non-stoichiometry can be described by the flowing defect reaction



Oxygen vacancies are formed and Fe⁺⁴ cations are reduced to Fe⁺³ at low oxygen partial pressures

$$K_{\text{ox}} = \frac{[O_{\text{O}}^x] [Fe_{Fe}^{\bullet}]^2}{[V_{\text{O}}^{\bullet\bullet}] [Fe_{Fe}^x]^2 P_{O_2}^{1/2}} \quad (6)$$

In order to maintain the fixed A/B ratio, the following equation must be maintained

$$[Fe_{Fe}^x] + [Fe_{Fe}^{\bullet}] + [Al_{Sr}'] = 1 \quad (7)$$

Kröger-Vink notation is used with Sr(+2) Fe(+4)O₃ as the reference state.

The experimental non-stoichiometry data as a function of pO₂ are fitted to equation (6) taking the equilibrium constant as a fitting parameter.

From equation (1) (3) (4) (7) we obtain

$$[Fe_{Fe}^{\bullet}] = 1 - 2\delta \quad (8)$$

$$[Fe_{Fe}^x] = 2\delta - x \quad (9)$$

If the set of concentration is accepted, we can insert $(V_{\text{O}}^{\bullet\bullet})$, (O_{O}^x) , (Fe_{Fe}^x) , and (Fe_{Fe}^{\bullet}) into equation (6) and find the oxygen partial pressure that corresponds to the equilibrium concentrations. The calculation is next performed for a new value of $(V_{\text{O}}^{\bullet\bullet})$ until all the concentration interval of interest has been covered.

3. Results and discussion

The simulations are normally made for an interval $[V_{\text{O}}^{\bullet\bullet}]$ which corresponds to the experimental data. Solutions are normally generated for a pO₂ range from 10⁻⁶ to 1 atom. The equilibrium constants used in the following are calculated using non-stoichiometric values from TG-data.[4][12][13]

3.1. Defect concentrations in Sr Fe_{1-x}Al_x O_{3-δ}

For the purpose of comparison, we chose to present for all species and in the Sam defects diagram the concentrations as a function of pO₂. Fig.1 shows the defect diagram for SFA10.

At high pO₂, Fe⁺³ ions are oxidized into Fe⁺⁴ and holes are the dominant defects. The electron concentration decreases while the hole concentration becomes comparable to the point defect concentration. Charge neutrality can only be maintained by decreasing the positively charged metal and increasing the positively charged vacancies.

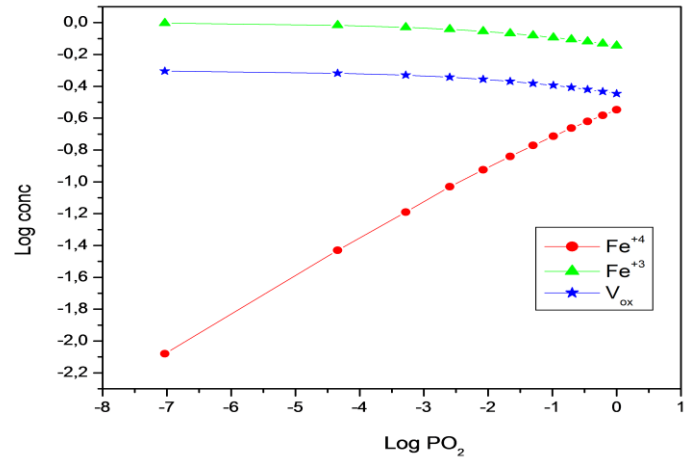


Fig. 1. Defect diagram for SFA10 at 1173K.

The relative carrier concentration for SFA10 as a function of pressure at different temperatures is shown in Fig. 2. The variation of Fe⁺⁴ for Sr Fe_{0.9} Al_{0.1} O₃ as a function of partial pressure calculated by Van Hassel et al.[24] is similar to the obtained results (Fig. 1) for SFA10. In the ionic compensation charge, the carrier concentration appears to be in agreement with

pO_2 dependence proposed by the model within the temperature range investigated (923K-1223K).

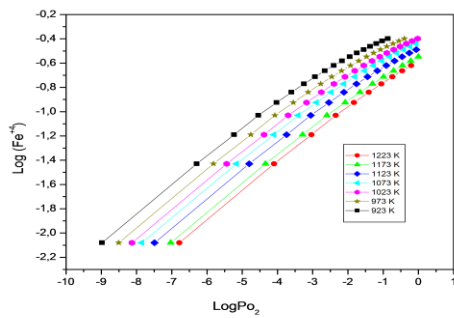


Fig. 2. Relative carrier concentration as a function of pO_2 and temperature for SFA10.

The effect of Al content at 1173 K on the carrier concentration is shown in Fig. 3. The relative carrier concentration appears to have a one-fourth power dependence on pO_2 in the region where oxygen compensation is expected ($pO_2 > 10^{-6}$ atm). The figure also indicates that the transition from ionic to electronic compensation occurs at relatively higher pO_2 as the Al content increases, as expected from the model.

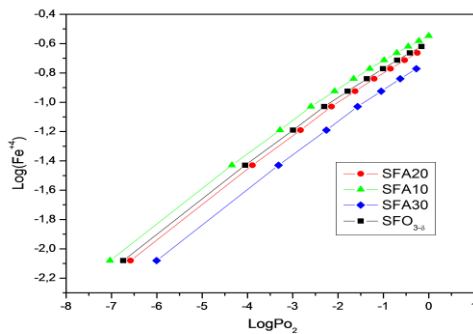


Fig.3. Relative carrier concentration as a function of pO_2 and composition at 1173k.

The calculated non-stoichiometry as a function of pO_2 for SFA10, SFA20 and SFA30 at 1173k, is presented in Fig. 4. At constant temperature, the pO_2 is higher for the composition with higher Aluminum content. The calculated non-stoichiometry isotherms are in good agreement with the reported thermo-gravimetry data and similar to those obtained for Al-doped $SrFeO_3$. These results conform very well to those obtained for the dependence of carrier concentration with pO_2 (Fig. 3).

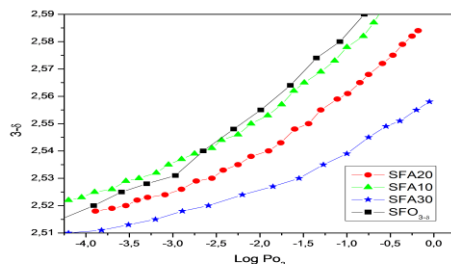


Fig.4. Simulated oxygen non-stoichiometry at 1173k for 3 compositions, SFA10, SFA20 and SFA30.

The effect of temperature on oxygen non-stoichiometry of SFA10 is shown in Fig. 5. A good agreement was obtained with the experimental TG data [4][12][13]. This result confirms the validity of the proposed defect model for SFA. For all cases, δ increases with increasing temperature and decreasing oxygen partial pressure. It is clear that it is much easier to form oxygen vacancies at high temperature. The same behavior was found in $(La, Sr)(Cr, M)O_{3-\delta}$ ($M=Ti, Mn$ and Fe) system [15][5][6]. This point defect model and itinerant electron model [3] described very well the non-stoichiometry behavior of SFA system.

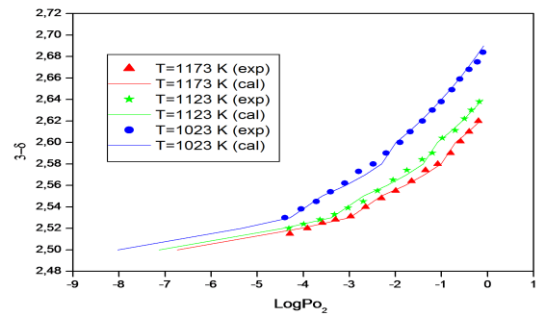


Fig.5. Simulated oxygen non-stoichiometry of SFA10 as a function of oxygen partial pressure at different temperatures.

3.2. Electrical conductivity

Depending on non-stoichiometry, the charge carriers in SFA may be either electrons, holes or both. Therefore, the general expression for the electrical conductivity must involve the components related to both electrons and holes:

$$(10)$$

Where q is the elementary charge, μ is the mobility and the subscripts correspond to the specific charge carriers. As seen from equation (1), both the reduced regime and the oxidized regime are governed by the same charge neutrality.

Fig. 6 present the dependence of the conductivity on oxygen partial pressure at different temperatures. A good agreement was obtained between the calculated conductivities presented by the solid lines and the experimental data [2][12] at different temperatures. This indicates clearly that the point defect model proposed describes well this material.

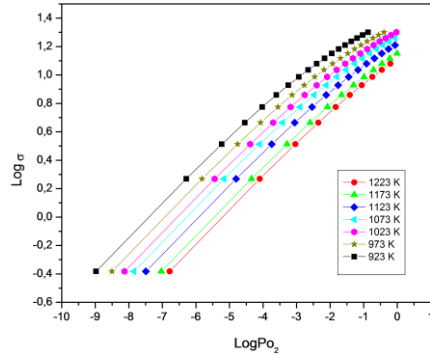


Fig. 6. Electrical conductivity of SrFe_{0.9}Al_{0.1}O_{3-δ} as a function of pO₂ at different temperatures.

The decrease of the electrical conductivity with increasing temperature reflects the decrease of the concentration of free electrons, holes and tetravalent Fe ions Fig. 2. The comparison of this behavior with oxygen non-stoichiometry measurements suggests that it is correlated with the increase in the concentration of Fe⁴⁺.

The effect of temperature on the conductivity for SFA10 is shown in Fig. 6. In the ionic compensation region, the electrical conductivity dependence on oxygen partial pressure proposed by this model is in good agreement with Meadowcroft's Work [21]. This behavior is similar to that observed in Al-doped SrFeO₃[25][26] and LSM[17]. As expected, the Figure further indicates that, in the intermediate pO₂ range, where electronic compensation predominates, the conductivity is independent of both temperature and pO₂. The transition from pO₂ dependence to independence shifts to higher oxygen partial pressure as the temperature of equilibration increases from 923-1223K. These results are in close agreement with the reported conductivity measurements[6][20][21]

Since the ionic conductivities of SFA(Fig. 7) are by several orders of magnitude smaller than the electronic conductivities [5][6][12], the experimentally determined total conductivities can in good approximation be considered as electronic conductivities. The thermoelectric power was found to be positive in SFA suggesting holes as the dominant charge carriers[5][16].

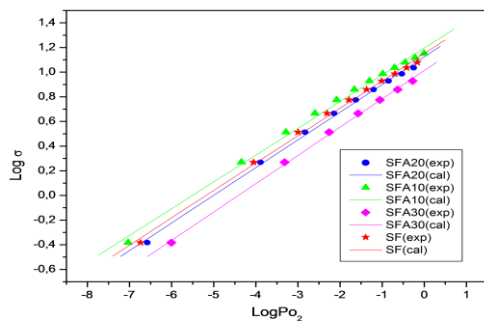


Fig.7. Conductivity isotherms at 1173K for three different compositions SFA10,SFA20 and SFA30.

Faber et al suggested that SrFe_{0.9}Al_{0.1}O_{3-δ} is a p type conductor and its conductivity arises from the presence of multivalent Fe ions due to Al doping [20].

The constant electrical conductivity that exists in the high pO₂ region may be easily understood if it is assumed that acceptors control the carrier concentration and that the electronic compensation predominates. In the lower pO₂ region, oxygen vacancies are formed and the electrical conductivity begins to decrease due to ionic charge compensation. The conductivity mechanism in acceptor-doped strontium iron is due, as mentioned in the literature, to small-polaron hopping irrespective of the kinds of dopants[27][28].

3.3. Thermodynamic consideration of the defect model

Some useful thermodynamic quantities such as the standard free energy charge, the standard entropy and the standard enthalpy charge for the reaction of equation (6). The chemical potential μ of oxygen in SFA oxide is equal to that of exterior gas

$$2\mu(\text{oxide}) = \mu(\text{gas}) \quad (11)$$

And we have

$$\mu(\text{gas}) = \mu^0(\text{gas}) + RT \ln P_{O_2} \quad (12)$$

The free molar energy of oxygen was given by the following equation

$$\Delta G_{O_2} = RT \ln P_{O_2} \quad (13)$$

$$\Delta G_0 = \Delta G_0^0 + (RT/2) \ln P_{O_2} \quad (14)$$

Using partial molar enthalpy, ΔH_o and partial molar entropy, ΔS_o we have

$$\Delta G_0 = \Delta H_0 - T \Delta S_0 \quad (15)$$

From equation (14) and (15), we obtain

$$\Delta H_0 = (R/2) \left(\frac{\partial \ln P_{O_2}}{\partial (1/T)} \right)_\delta \quad (16)$$

$$\Delta S_0 = -1/2 \left(\frac{\partial (RT \ln P_{O_2})}{\partial (T)} \right)_\delta \quad (17)$$

These quantities are calculated SF and SFA using the equilibrium constants versus oxygen nonstoichiometry δ Fig 8,9. The values of partial molar enthalpy indicate that oxygen incorporation in the lattice is favorable for rich compositions with Aluminum. The enthalpy of the reaction was obtained from the slope of the Arrhenius plot. The values depend on the composition x and are

relatively close to those obtained for $\text{SrFe}_{1-x}\text{Al}_x\text{O}_{3-\delta}$ [29]. The slight difference from values of δ and for the same Al-dopant LaFeO_3 [19], is due to interaction between defects that we do not take into account in the present defect model. The changes in standard enthalpy and standard entropy show a composition dependence with acceptor-dopant.

From Fig. 8. One can observe an decrease of molar partial entropy versus oxygen nonstoichiometry which indicates that oxygen vacancies in SFA are randomly distributed in the crystal lattice.

This remark was supported by the variation of the molar partial entropy with δ . In fact Fig. 9. Shows a slight decrease of enthalpy with increasing nonstoichiometry.

From these results, the standard enthalpy depend strongly on composition, so the Al concentration charge. This behavior was also suggested for $\text{SrFe}_{1-x}\text{Al}_x\text{O}_{3-\delta}$ and $\text{SrFe}_{1-x}\text{Ga}_x\text{O}_{3-\delta}$ Mizusaki [18], which is in good agreement with the non stoichiometry data [29] [30].

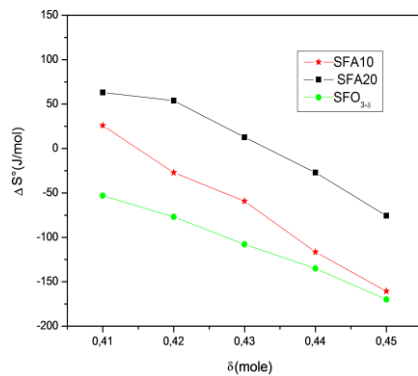


Fig. 8. Partial molar entropy versus oxygen nonstoichiometry δ for SFA10.

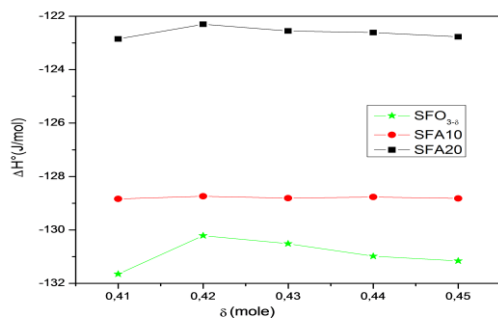


Fig. 9. Partial molar enthalpy versus oxygen nonstoichiometry δ for SFA10.

4. Conclusion

The data obtained from TG experiments support the proposed defect model for the oxidation behavior of $\text{SrFe}_{1-x}\text{Al}_x\text{O}_{3-\delta}$. This model indicates that at high $p\text{O}_2$ electronic compensation occurs by a transition of Fe^{+3} to Fe^{+4} , whereas ionic compensation takes place at lower

$p\text{O}_2$ by the formation of oxygen vacancies. The oxygen nonstoichiometry of B-site mixed $\text{Sr}(\text{Fe},\text{Al})\text{O}_3$ strongly depends on the composition of B-site dopants. The stability of the oxide increases for lower Al content at high $p\text{O}_2$.

The conductivity of SFA system was mainly due to p-type charge carriers Fe^{+4} which act as traps.

The changes in partial molar enthalpy and entropy show a composition dependence with acceptor/donor-dopants partial molar enthalpies values indicate that oxygen dissolution in the lattice is favorable for Al doped on B-site.

References

- [1] Liu, J, Co, A, C, Paulson, S, Birss, 2006, V, I, Solid State Ionics, p.177,377.
- [2] H, Iwahara, T, Esaka and T. Sato, J. Solid State Chem, 1981, p.39,173.
- [3] Baumann, F, S, Fleig, Habermeier, H, U, Maier, 2006, J, Solid State Ionics, p.177,1071.
- [4] Lankhorst, M, H, R, Bouwmeester, H, G, M, Verweij, H, 1997, J, Solid State Chem, p.133,555.
- [5] Omari, M, Chadli, I, Belaidi, S, Turk, J, Chem, 2004, p.28,535.
- [6] Omari, M, Diafi, M, Adaika, K, Jordan Journal Of Chemistry ol, 5No3, 2010, p.271-282.
- [7] Mineshige, A, Abe, J, Kobune, M, Uchimoto, Y, Yazawa, T, 2006, Solid State Ionics, 177, 1803.
- [8] Bucher, E, Sitte, W, Caraman, G, B, Cherepanov, V, A, A, ksenova, T, V, Ananyev, M, V, 2006, Solid State Ionics, p.177,3109.
- [9] Spinolo, G, Anselmi-Tamburini U, Ber, Bunsenges, 1995, Phys. Chem, p.99,87.
- [10] Spinolo, G, Anselmi-Tamburini U, and Ghigna, P, 1997, Zeitung Fur Naturforschung, p.A52, 629.
- [11] Poulsen, F, W, J, Solid State Chem, 1999, p.143,115.
- [12] Wang, S, Katsuki, M, Dokiya, M, Hashimoto, T, 2003, Solid State Ionics, p.159,71.
- [13] Mineshige, A, Izutsu, J, Nakamura, M, Nigaki, K, Ade, J, Kobune, M, Fujii, S, Yazawa, T, 2005, Solid State Ionics, p.176,1145.
- [14] Kröger, F, A, and Vink, H, J, Solid State Physics, eds, dyF, Seitz and D, Turnbull, Academic Press, New York, 1956p., 3,307.
- [15] Oishi, M, Yashiro, K, Sato, K, Mizusaki, J, Kawada, T, J, Solid State Chem, 2008, p.181,3177.
- [16] Swierczek, K, Solid State Ionics, 2008p., 179,126.
- [17] F, w, Poulsen, Solid State Ionics, 2000, p.129,145.
- [18] J, Mizusaki, M, Yoshihiro, S, Yamauchi and K, Fueki, J, Solid State Chem, 1987p.67,1.
- [19] J, Mizusaki, S, Yamauchi, K, Fueki and A, Ishikawa, J, Solid State Chem, 1984, p.12,119.
- [20] J, Faber, M, Mueller, W, Procarione, A, Aldred and H, Knott, Conference on High Temperature Science Related to Open Cycle, Cool Fired MHD Systems. Argonne National Laboratory, Argonne, IL, April 1977.
- [21] D, B, Meadowcroft, Br, J, Appl, Phys 1969, p.9,1225.
- [22] H, Uchida, H, Yoshikawa and H, Iwahara, 1989, Solid State Ionics, 35,229.
- [23] T, Schober, W, Schilling and H, Wenzl, Solid State Ionics, 1996, p.86-88,653.
- [24] B, A, VanHassel, T, Kawada, N, Sakai, H, Yokokawa, M, Dokiya and H, J, M, Bouwmeester Solid State Ionics, 1993, p.66,295.
- [25] I, Yasuda and T, Hikita, 1993, J, Electrochem, Soc, 140,1699-1704.
- [26] H, Kamata, Y, Yononemura, J, Mizusaki, H, Tagawa, K, Naraya and T, Sasamoto, J, Phys, Chem, Solids, 56, 1995, p.943-50.

- [27]D,P, Karim and A, T, Aldred, Phys, Rev, B, 20,1255,1979.
- [28]J,B, Webb, M, Sayer and A, Mansingh, Can, J,1955, Phys, 55,1725.
- [29]J,Mizusaki,M,Yoshihiro,S,Yamauchi and K,Fueki,J,Solid State Chem,58,257(1985).
- [30]J,Mizusaki, Y,Mima,S,Yamouchi and K,Fueki,J,1989,Solid State Chem, 80,102.